frontiers | Frontiers in Rehabilitation Sciences

ORIGINAL RESEARCH
published: 31 May 2022
doi: 10.3389/fresc.2022.910068

IVIM Imaging of Paraspinal Muscles Following Moderate and High-Intensity Exercise in Healthy Individuals

Erin K. Englund[1,2†], David B. Berry[1,3], John J. Behun[1], Samuel R. Ward[1,4,5], Lawrence R. Frank[4] and Bahar Shahidi[1]*

[1] Department of Orthopaedic Surgery, University of California, San Diego, La Jolla, CA, United States, [2] Department of Radiology, University of Colorado Anschutz Medical Campus, Aurora, CO, United States, [3] Department of Nanoengineering, University of California, San Diego, La Jolla, CA, United States, [4] Department of Radiology, University of California, San Diego, La Jolla, CA, United States, [5] Department of Bioengineering, University of California, San Diego, La Jolla, CA, United States

OPEN ACCESS

Edited by:
Andrew C. Smith, University of Colorado, United States

Reviewed by:
Stephan Bodkin, University of Colorado Anschutz Medical Campus, United States
Adam Kuchnia, University of Wisconsin-Madison, United States

***Correspondence:**
Bahar Shahidi
bshahidi@health.ucsd.edu

†Present address:
Erin K. Englund, Department of Radiology, University of Colorado Anschutz Medical Campus, Aurora, CO, United States

Specialty section:
This article was submitted to Rehabilitation for Musculoskeletal Conditions, a section of the journal Frontiers in Rehabilitation Sciences

Received: *31 March 2022*
Accepted: *09 May 2022*
Published: *31 May 2022*

Citation:
Englund EK, Berry DB, Behun JJ, Ward SR, Frank LR and Shahidi B (2022) IVIM Imaging of Paraspinal Muscles Following Moderate and High-Intensity Exercise in Healthy Individuals. Front. Rehabilit. Sci. 3:910068. doi: 10.3389/fresc.2022.910068

Background: Quantification of the magnitude and spatial distribution of muscle blood flow changes following exercise may improve our understanding of the effectiveness of various exercise prescriptions. Intravoxel incoherent motion (IVIM) magnetic resonance imaging (MRI) is a technique that quantifies molecular diffusion and microvascular blood flow, and has recently gained momentum as a method to evaluate a muscle's response to exercise. It has also been shown to predict responses to exercise-based physical therapy in individuals with low back pain. However, no study has evaluated the sensitivity of IVIM-MRI to exercise of varying intensity in humans. Here, we aimed to evaluate IVIM signal changes of the paraspinal muscles in response to moderate and high intensity lumbar extension exercise in healthy individuals.

Methods: IVIM data were collected in 11 healthy volunteers before and immediately after a 3-min bout of moderate and high-intensity resisted lumbar extension. IVIM data were analyzed to determine the average perfusion fraction (f), pseudo-diffusion coefficient (D*), and diffusion coefficient (D) in the bilateral paraspinal muscles. Changes in IVIM parameters were compared between the moderate and high intensity exercise bouts.

Results: Exercise increased all IVIM parameters, regardless of intensity ($p < 0.003$). Moderate intensity exercise resulted in a 11.2, 19.6, and 3.5% increase in f, D* and D, respectively. High intensity exercise led to a similar increase in f (12.2%), but much greater changes in D* (48.6%) and D (7.9%).

Conclusion: IVIM parameter increases suggest that both the moderate and high-intensity exercise conditions elicited measurable changes in blood flow (increased f and D*) and extravascular molecular diffusion rates (increased D), and that there was a dose-dependence of exercise intensity on D* and D.

Keywords: intravoxel incoherent motion (IVIM), exercise, paraspinal muscle, MRI, exercise intensity

INTRODUCTION

Perfusion to skeletal muscle is required to facilitate oxygen and nutrient delivery as well as removal of metabolic waste products. When skeletal muscle undergoes contraction, blood flow to muscle increases substantially, with perfusion increasing from ∼3–5 mL/min/100 g at rest (1) to 80 mL/min/100 g or more following exercise (2–5). Mechanisms to increase blood flow involve decreasing vascular resistance through vasodilation of the supplying arteries and arterioles and increasing the vascular recruitment at the level of the capillaries, essentially leading to an expansion of the available capillary surface area for exchange of oxygen between blood and muscle (6, 7).

Non-invasive measurement of whole muscle blood flow both at rest and in response to exercise using magnetic resonance imaging (MRI) is of great interest. Intra-Voxel Incoherent Motion (IVIM) is an MRI technique sensitive to perfusion (8) that has gained interest as a strategy to evaluate blood flow in skeletal muscle (9). IVIM uses diffusion-weighted MR images over a wide range of diffusion sensitivities or b-values, sensitizing the images not only to diffusion but also microvascular blood flow (so-called pseudo-diffusion) (10). The measured data are then fit to a bi-exponential model that describes the contribution of motion in the microvasculature (described by the pseudo-diffusion coefficient, D*) and extravascular spaces (described by the molecular diffusion coefficient, D), weighted by the intravascular signal fraction (f) to the signal decay. Thus, these coefficients provide insight into the relative microvascular blood volume (f) as well as the net displacement of MR-visible water molecules located in the intravascular (D*) and intracellular (D) spaces within a given voxel of the imaging data.

Thus, MRI can not only provide key information on muscle health and adaptive capacity (11–13), but also spatially sensitive information on regions of muscle that have activation impairments in a way that standard measures of muscle activation (e.g., electromyography) cannot (14–16). Identifying these impairments is essential to optimizing function and performance in both healthy individuals and individuals undergoing exercise-based rehabilitation for pain or injury. The ability to use an MRI technique that identifies activation impairments can provide key information on the physiological mechanisms underlying reduced activation in individuals with both healthy and pathological muscle (e.g., pain, disuse, denervation). This information can be used to inform targeted treatments in a patient-specific manner. For example, recently, Shahidi et al. identified perfusion-based impairments in paraspinal muscles of individuals with a history of low back pain after an acute bout of exercise (17). Further, the magnitude of the blood flow response the acute bout of exercise significantly predicted successful reduction in back-pain related disability with a longer-term exercise-based rehabilitation program targeting the paraspinal muscles of interest. Given that individuals with low back pain have been shown to demonstrate changes in muscle health such as atrophy, fibrosis, and fatty infiltration, this technique may provide useful information on pathologies with similar phenotypes. It may also allow clinicians to identify patients who are most likely to successful with exercise-based physical therapy and provides a physiological basis for future research on potential alternative management strategies for those who do not demonstrate the expected response.

Prior studies have demonstrated the ability of IVIM to detect blood flow-related changes in muscle following exercise in muscles of the upper (18–21) and lower extremities (22–25), and back (26, 27). Each of these studies measured the IVIM response to a single, high-intensity exercise stimulus, likely eliciting a maximal hyperemic response. An evaluation of the sensitivity of IVIM to detect blood flow changes to varied exercise intensities in humans has not been performed. Therefore, the purpose of this study was to compare the IVIM results in response to moderate and high intensity exercise to evaluate the ability of IVIM to detect dose-dependent blood flow changes in healthy individuals. We hypothesize that IVIM based measurements of perfusion will be sensitive to paraspinal blood flow changes following moderate and high-intensity lumbar extension exercise in a dose-dependent manner.

METHODS

Participants

The University of California San Diego's Institutional Review Board approved all experimental procedures. Each subject provided informed consent prior to his or her participation, and all study procedures were conducted according to the ethical principles set forth in the Belmont Report. Healthy subjects were recruited from the surrounding community. Potential participants were excluded if they reported a history of low back pain, had prior injuries or surgery to the lumbar spine region, had any contraindication to exercise or to MR imaging (e.g., metal implants, claustrophobia). A subset of the individuals enrolled in the present study also participated in a previously published study (17). Each subject came to the laboratory for two experimental sessions on different days—a minimum of 72 h apart—during which identical MR imaging was obtained before and after either a high or moderate intensity resisted lumbar extension exercise bout.

Imaging and Exercise Protocol

The experimental protocol is illustrated in **Figure 1**. All imaging was performed on a 3.0T MR imaging system (GE MR 750, GE Healthcare; Waukesha, WI) with a CTL phased-array spine coil for signal reception. Subjects were positioned head-first, supine and centered at ∼ the third or fourth lumbar vertebrae (L3/L4). IVIM data were collected at rest (after ∼10–15 min in the supine position) and immediately after a bout of moderate or high intensity bout of resisted lumbar extension exercise performed on a lumbar extension machine (Nautilus Evo, Nautilus Inc.) outside the scanner. For the high-intensity exercise, individuals were instructed to target a perceived exertion (RPE) of 6–8 out of 10 on a modified Borg Scale by self-paced exercise with the load set to 60% of their body weight. For moderate-intensity exercise, the targeted RPE was 3–4 out of 10, with the load set to 40% of their body weight. For both intensities, participants were instructed to exercise for ∼3 min, or whenever they reached the

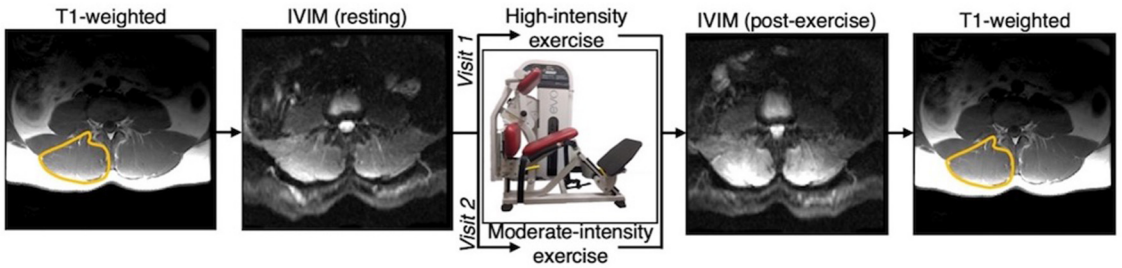

FIGURE 1 | Overview of experimental design. Participants were scanned at rest and following either a moderate or high intensity resisted lumbar extension exercise paradigm. Moderate and high intensity exercise sessions were performed on two separate days. T1-weighted anatomical reference images were acquired before and after the pre- and post-exercise IVIM data, respectively, and used to define the paraspinal muscles bilaterally.

targeted RPE. The subject immediately returned to the scanner for post-exercise imaging (**Figure 1**).

Resting and post-exercise IVIM data were identically acquired with an axial, multi-slice, 2D, diffusion-weighted, spin echo EPI with: FOV = 256 × 256 mm^2, slice thickness = 8 mm, 22 slices covering the entire lumbar spine from L1 to S1, acquisition matrix = 128 × 128, TR/TE = 2,295/52.5 ms, flip angle = 90°, spatial-spectral fat saturation, averages = 4, and 3 directions of diffusion encoding with b-values of 0, 10, 20, 40, 70, 110, 160, 220, 300, 400, 500, 600, and 700 s/mm^2, yielding a total acquisition time of 347 s. The pulse sequence diagram is shown in **Figure 2**.

Image Analysis

As described previously (17), diffusion-weighted images were preprocessed with phase and distortion correction using TOPUP (28, 29) and subsequently denoised using a principal component analysis filter (30). Data were spatially smoothed with a 2D median filter with a 3-voxel radius, and then averaged over the 3 diffusion encoding directions and the 4 temporal repeats for each b-value.

Given the varied strength of the diffusion-weighting gradients, the voxelwise signal intensities as a function of b-value will be sensitive to the underlying microscopic motion. As the scale of motion in the microvasculature vs. intracellular spaces differs substantially, a bi-exponential model can be used that describes both the contribution of motion in the microvasculature (described by the pseudo-diffusion coefficient, D*) and extravascular spaces (described by the molecular diffusion coefficient, D) to the signal decay as:

$$S(b)/S_0 = (1 - f)e^{-bD} + f\,e^{-bD^*} \quad (1)$$

where $S(b)/S_0$ is the measured signal at each b-value, normalized by the non-diffusion weighted acquisition, D the molecular diffusion coefficient, D* the pseudo-diffusion coefficient, and f is the perfusion fraction, representing the fractional volume of blood in each voxel.

The scale of mean squared displacement of water molecules in the intra- vs. extravascular spaces differs by ∼ an order of magnitude. Extravascular diffusion is governed by Brownian motion, whereas the displacement in the intravascular space is related to both Brownian motion and the convective flow of blood in the capillaries (10). Separation of the diffusion and pseudo-diffusion coefficients is therefore possible because contribution from intravascular motion (i.e., D*) to the overall signal decay at high b-values is negligible, meaning that the signal decay at high b-values is governed only by molecular diffusion, D. Here, a three-step constrained fitting approach was used to solve for parameter maps of the coefficients D, f, and D* from the slice-wise IVIM data (**Figure 3**). First data obtained at b >200 s/mm^2 (i.e., the high b-value regime) were log-transformed and fit to a first-order polynomial as: $\ln\left(S\left(b > 200\right)\right) = -bD + S_0^{'}$ in order to obtain D. S_0', the y-intercept, was then used to calculate the perfusion fraction as: $f = 1 - S_0^{'}/S_0$. Once f and D were determined from these first two steps, data from all b-values were used to solve (eq. 1) for D* using a non-linear least-squares fitting approach (31). Boundary conditions were applied for all parameters using the following constraints: 0–0.5 for f, 1.5–500 × 10^{-3} mm^2/s for D*, and an upper bound of 2.5 × 10^{-3} mm^2/s (the coefficient of free diffusion of water at body temperature) for D. In addition, from the resulting parametric maps, the product of f and D* (fD*) was computed, a parameter most closely related to microvascular blood flow (32).

T1-weighted anatomical reference images were obtained prior to the resting IVIM data and following the IVIM images after exercise. These T1-weighted images were acquired with the same FOV, slice thickness, and image orientation as the IVIM data (**Figure 1**). Regions of interest (ROIs) were defined by a single observer on the T1-weighted images for the bilateral erector spinae and multifidus muscles combined, using previously described definitions of the muscle boundary (33). ROIs were then transferred to the IVIM parameter maps then eroded to avoid voxels that may be impacted by partial volume artifacts. Data within the ROIs were averaged across the lumbar extensor muscles from L1 to S1 to obtain the mean f, D, and D* at rest and following exercise for each participant.

Statistical Analysis

Two-way within-subjects repeated-measures analysis of variance (RM-ANOVA) tests were used to compare IVIM parameters before and after exercise between the moderate- and high-intensity exercise bouts. *Post-hoc* paired samples tests were used

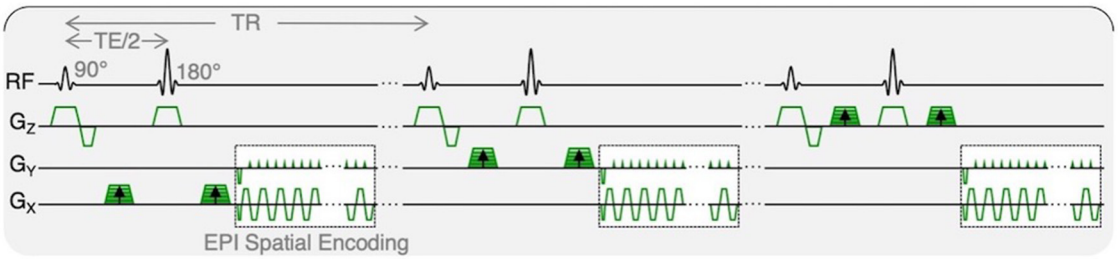

FIGURE 2 | IVIM pulse sequence diagram. Diffusion-weighted MR data were acquired with trace weighting and varying b-values, contributing to varied motion sensitivity. Total acquisition time was 347 s.

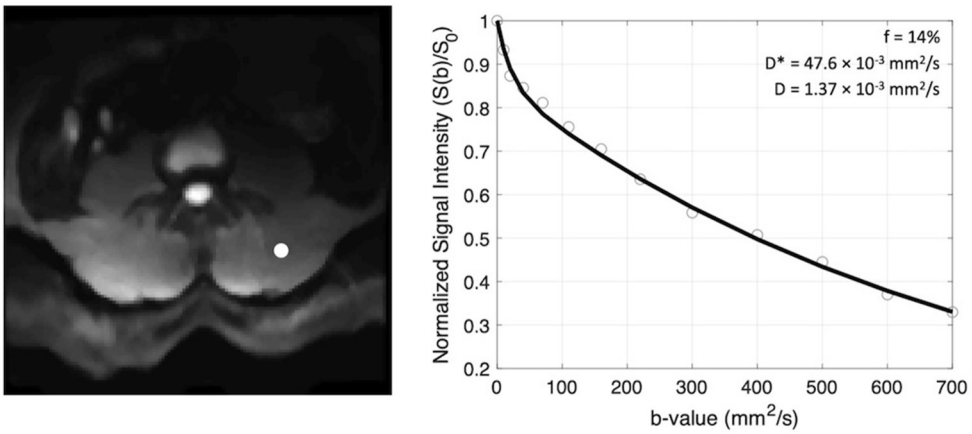

FIGURE 3 | Example of signal decay as a function of b-value (right) shown for the voxel indicated by the white circle on the left panel. The normalized signal intensity data are fit to a bi-exponential function and coefficients f, D*, and D are recorded.

to evaluate significant differences among individual exercise intensities (e.g., resting vs. following moderate intensity exercise). *Post-hoc* tests were corrected for multiple comparisons using the Sidak method. In order to determine parameter estimates reflecting the amount of change in IVIM measures distinguishing high vs. moderate intensity exercise, univariate regressions were performed for the change in parameters from baseline against the exercise state (moderate and high) for significant variables. In all cases, a p-value of 0.05 was considered statistically significant. All statistics were performed using SPSS Statistics (Version 21, IBM, Armonk, NY). All data are reported as mean ± standard deviation unless otherwise noted.

TABLE 1 | Results of exercise protocols for moderate and high intensity exercise paradigms.

	Moderate intensity exercise	High intensity exercise
Relative perceived exertion	3.4 (0.9)	7.1 (1.0)
Resistance weight (kg)	31.3 (7.2)	47.6 (9.2)
Exercise duration (s)	161 (34)	175 (20)
Time to start of IVIM acquisition (s)	182 (74)	164 (40)

All data shown as mean (standard deviation).

RESULTS

A total of twelve healthy individuals (6 male, age range = 21–63 years old) were recruited to participate in this study. Data from one participant was excluded due to image artifacts. In the remaining 11 participants, all participants were able to achieve the targeted RPE for both moderate (RPE = 3.4 ± 0.9) and high intensity (RPE = 7.1 ± 1.0) exercise (**Table 1**). By design, there were significant differences of RPE and resistance weight between the moderate and high-intensity exercise bouts, however differences were not observed between exercise duration (p = 0.10) or time between the end of exercise and the start of the post-exercise IVIM acquisition ($p = 0.65$).

Representative parameter maps for each of the IVIM coefficients are shown in **Figures 4–7** at rest and following moderate and high-intensity exercise. These images demonstrate the increase of blood flow and molecular diffusion brought about by exercise. The IVIM parameters at rest were not significantly different between visits (f: $p = 0.14$; D*: $p = 0.71$; fD*: $p = 0.61$; D: $p = 0.93$). Overall, both moderate and high intensity exercise elicited an increase in perfusion fraction ($p = 0.003$) and mean

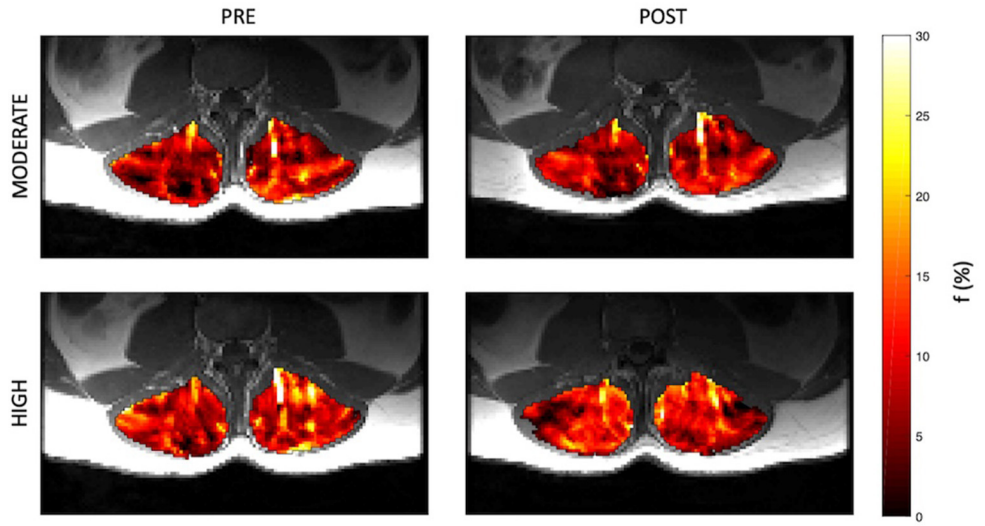

FIGURE 4 | Representative parameter maps of perfusion fraction, f, before and after both moderate (top) and high (bottom) intensity resisted lumbar extension exercise.

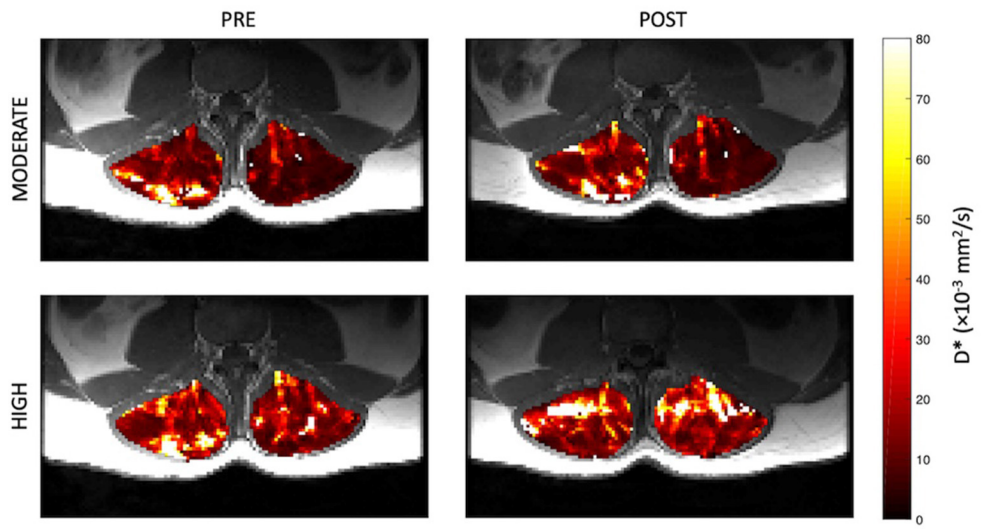

FIGURE 5 | Representative parameter maps of pseudo-diffusion coefficient, D*, before and after both moderate (top) and high (bottom) intensity resisted lumbar extension exercise.

squared displacement of water molecules in the intravascular (D*: $p < 0.0001$; fD*: $p < 0.0001$) and extravascular (D: $p < 0.0001$) spaces (**Figure 8**; **Table 2**). Moderate intensity exercise led to a 11.2 ± 12.9% increase in f, 19.6 ± 21.7% in D*, 33.0 ± 26.4% in fD*, and 3.5 ± 2.4% in D. High-intensity exercise yielded a 12.2 ± 16.9% increase in f, 48.1 ± 13.9% in D*, 48.6 ± 23.4% in fD*, and 7.9 ± 1.9% in D. The RM-ANOVA revealed a significant interaction between time (e.g., pre-post exercise) and exercise intensity for both D* ($p = 0.004$) and D ($p = 0.001$), but not f ($p = 0.88$) or fD* ($p = 0.20$). *Post-hoc* tests revealed a significant difference between exercise intensity post exercise for both D ($p = 0.002$) and D* ($p = 0.015$) but not f ($p = 0.177$) or fD* ($p = 0.144$). Univariate regression models revealed that a mean ± SE increase of 4.46 ± 0.91% in D, and an increase of 28.56 ± 7.77% in D* reflects the expected increase in exercise intensity (relative to baseline) between moderate and high ($p < 0.001$, and $p = 0.001$, respectively).

DISCUSSION

The results of this study demonstrate that IVIM coefficients are stable at rest between days and that these parameters

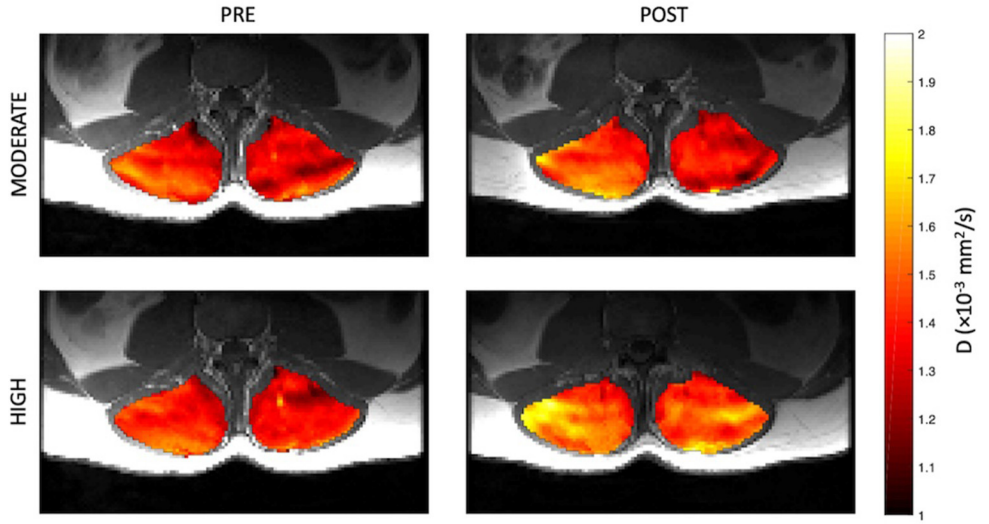

FIGURE 6 | Representative parameter maps of diffusion coefficient, D, before and after both moderate (top) and high (bottom) intensity resisted lumbar extension exercise.

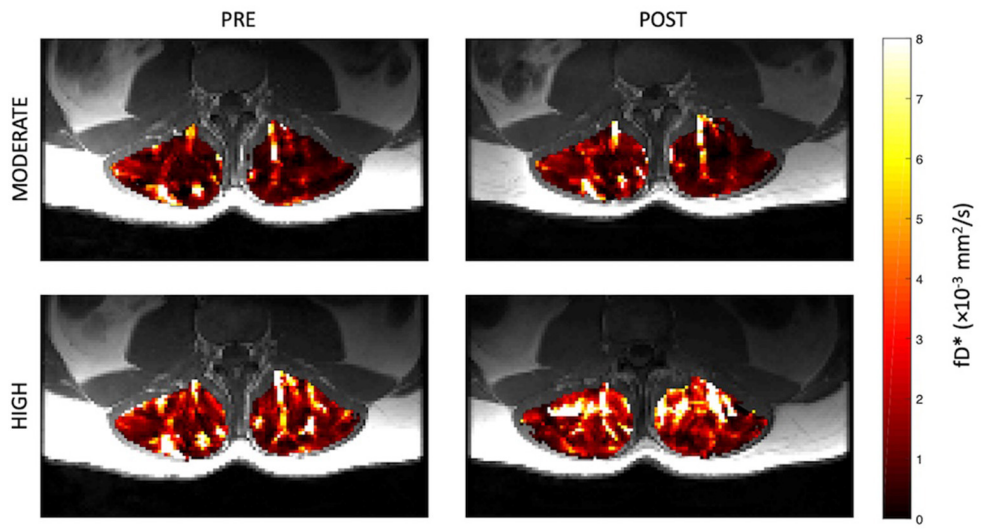

FIGURE 7 | Representative parameter maps of fD* before and after both moderate (top) and high (bottom) intensity resisted lumbar extension exercise.

are sensitive to paraspinal microvascular blood flow and molecular diffusion changes in a dose-dependent capacity in response to an acute bout of resisted lumbar extension exercise. In accordance with our hypothesis, we found that high-intensity exercise elicited a larger magnitude of changes in IVIM coefficients D* and D compared to moderate-intensity exercise, despite quite limited differences in RPE between the two exercise bouts. Interestingly, while exercise led to an increase in f and fD*, there was no difference found between the moderate and high-intensity exercise conditions. Prior to this investigation, a direct comparison of the IVIM response to varying exercise intensities in the same human subjects, regardless of muscle of interest had not yet been performed.

The increases in each parameter with exercise observed, are in agreement with prior studies investigating the exercise response of the paraspinal muscles to a single intensity of exercise with IVIM. Hiepe et al. evaluated the change in IVIM parameters ∼2 min after an isometric back extension exercise that was perceived as hard, reporting an increase in both D and f (27). Similarly, Federau et al. compared the change in IVIM parameters after dynamic lumbar extension exercise performed until exhaustion in both healthy individuals and patients with adolescent idiopathic scoliosis (26). In healthy individuals, they

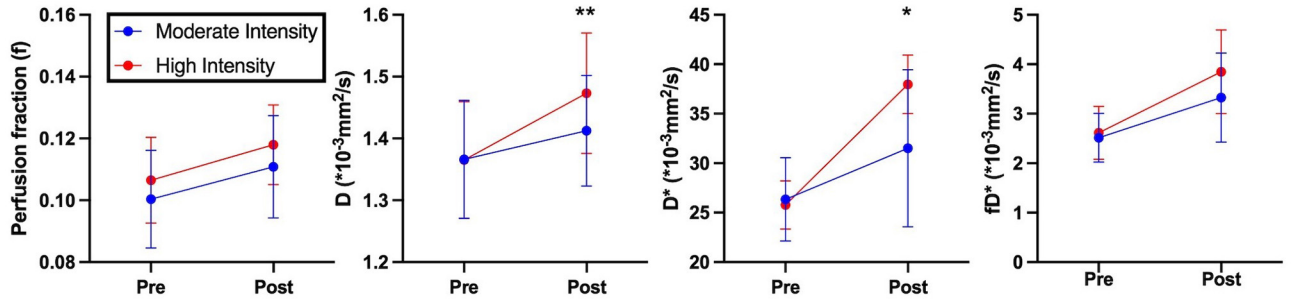

FIGURE 8 | IVIM based perfusion measurements of volunteers pre- and post- exercise. Blue indicates moderate intensity exercise. Red indicates high intensity exercise. Asterisks indicate significant differences in perfusion measurements post exercise between moderate and high intensities (*$p < 0.05$, **$p < 0.01$).

TABLE 2 | Results of IVIM coefficients at rest and in response to moderate and high intensity exercise.

	Moderate intensity exercise			High intensity exercise		
	Resting	***Post-exercise***	***P-value***	***Resting***	***Post-exercise***	***P-value***
f (%)	10.0 (1.6)	11.1 (1.7)	0.018	10.6 (1.4)	11.8 (1.3)	0.037
D* ($\times 10^{-3}$ mm^2/s)	26.3 (4.2)	31.5 (7.9)	<0.001	25.8 (2.4)	38.0 (3.0)	<0.001
D ($\times 10^{-3}$ mm^2/s)	1.37 (0.10)	1.31 (0.09)	0.020	1.37 (0.09)	1.47 (0.10)	<0.001
fD* ($\times 10^{-3}$ mm^2/s)	2.52 (0.49)	3.33 (0.90)	0.004	2.62 (0.53)	3.85 (0.84)	<0.001

All data shown as mean (standard deviation).

found a significant increase in all IVIM parameters in response to the high-intensity exercise protocol. In a previous study including a subset of individuals enrolled in the present study (17), the response to high-intensity exercise was compared between people with a history of low back pain and healthy controls. The results of that study illustrated the sensitivity of IVIM to detect clinically significant changes in the blood flow response to exercise between individuals with and without low back pain. A study by Lyu et al. investigated the IVIM response to varying exercise programs and durations at serial timepoints after exercise in Sprague-Dawley rats (34). However, this experimental design may not be sensitive to the acute effects of exercise given that their shortest post-exercise data were collected 30 min after exercise cessation. Nevertheless, significant differences between D and D* were observed between exercise protocols, f was not reported in this study.

The increase in molecular diffusion coefficient in response to exercise has been previously attributed to changes in myofiber diameter or tissue heating. While not directly evaluated with IVIM, prior studies have demonstrated a sensitivity between Blood Oxygen Level Dependent (BOLD) imaging, T2-weighted imaging, or diffusion-weighted imaging with the degree of exercise intensity. For example, T2-weighted imaging has been shown to be directly related to exercise intensity (35) and exercise-related glucose uptake measured via FDG-PET in healthy individuals (36). Along with diffusion imaging, T2-weighted imaging has been shown to be sensitive to increased intra- and extracellular fluid shifts, increased blood flow, and microvascular flow (37, 38). However, Froeling et al. demonstrated that while traditional T2-weighted fat suppressed MR images were unable to detect changes in different muscles after prolonged endurance exercise (marathon running), diffusion tensor imaging (DTI) detected intermuscular diffusivity changes, suggesting that diffusion-based imaging may be more sensitive to exercise-induced fluid shifts (39). Similarly, BOLD imaging is thought to be sensitive to blood oxygenation level changes in response to varying exercise intensities, although some data suggests that BOLD signal is less sensitive at higher exercise intensities (40). Although these alternative imaging methods have been used to evaluate differences in exercise intensity with varying levels of sensitivity, the ability to utilize a technique that can distinguish between healthy and pathological states is also of value. Because IVIM provides information specific to capillary blood flow, it provides unique information that is not available using the aforementioned MRI techniques. Given that impairments in capillary function or density are a common feature of pathological muscle in a variety of conditions including spine pathology, diabetes, peripheral arterial disease, and even across the spectrum of aging, the ability to utilize a technique that is sensitive to the capillary function in the context of an exercise challenge allows for potentially broad applicability in commonly seen patient populations.

Contrary to our hypothesis, we did not observe the same dose-dependent increase in perfusion fraction that was observed for the other parameters. This may be due to the way that the control of blood flow at the local level is mediated by microvascular units, a group of ∼2–20 capillaries fed by a single terminal arteriole. Microvascular units represent the smallest functional unit of blood flow regulation. At submaximal exercise intensity, only a fraction of myofibers, dispersed throughout the muscle,

are activated, as governed by individual motor units. Given the spatial incongruity between motor units (dispersed throughout the muscle) and microvascular units (locally constrained), activation of additional motor units with increasing exercise intensity may not lead to a substantial change in the fraction of blood in the capillaries. This relationship between the spatial organization of blood flow control vs. myofiber activation is one potential explanation for the lack of effect of exercise intensity on f. Increasing exercise intensity would, however, cause additional vasodilation of the feeding arteries and resistance arterioles, leading to faster transit of blood throughout the capillaries, hence an increase in D*. Physiologic modeling and phantom experiments could help to elucidate the relationship between changes in blood flow velocity, blood volume, and molecular diffusion on the measured IVIM signal. In addition, the inclusion of a measurement of blood oxygenation at the tissue level would help to fully understand the relationship between the metabolic demand of exercise and the microvascular and musculoskeletal responses.

Our study is not without limitations. While results demonstrated an effect of exercise intensity on the IVIM coefficients D and D*, only two exercise intensities were evaluated. Additional time points following exercise cessation as well as inclusion of more steps of exercise intensity would help to fully define the relationships that were observed. Some prior literature evaluating other imaging techniques to measure exercise response has included concurrent physiologic measures representing muscle activation, including near infrared spectroscopy (NIRS) for blood oxygenation, pH measures, and electromyography (41, 42). Follow-up studies employing multiparametric imaging and complementary physiologic measures would help to better understand the methodologic responses and physiologic underpinning of the observed IVIM signal changes. Additionally, although our group has demonstrated in a prior study that there are differences in IVIM-based exercise responses between healthy individuals and those with low back pain, we did not evaluate how pain, disease, or aging may differentially impact these responses.

CONCLUSION

Our study is the first to evaluate the effect of varying exercise intensities on muscle perfusion and diffusion using IVIM MRI in healthy human paraspinal muscle. We found that high-intensity resistance exercise of the lumbar paraspinal muscles elicited a larger magnitude of changes in IVIM coefficients D* and D, but not f or fD* as compared to moderate-intensity exercise. Further studies are needed to validate these findings against physiological standards.

DATA AVAILABILITY STATEMENT

The raw data supporting the conclusions of this article will be made available by the authors, without undue reservation.

ETHICS STATEMENT

The studies involving human participants were reviewed and approved by University of California San Diego Institutional Review Board. The patients/participants provided their written informed consent to participate in this study.

AUTHOR CONTRIBUTIONS

BS, SW, and LF designed the study. BS and EE collected data. BS, EE, DB, and JB contributed to data processing and analysis. BS, EE, SW, LF, and DB interpreted the data. BS, EE, SW, LF, DB, and JB wrote and approved the manuscript. All authors contributed to the article and approved the submitted version.

FUNDING

Work for these experiments was funded by the National Institutes of Health grants R03HD094598 (awarded to BS) and R01AR070830 (awarded to SW and LF). Support for time writing this manuscript was provided to EE on NIH/NCATS Colorado CTSA Grant KL2TR002534.

REFERENCES

1. Barrett EJ, Rattigan S. Muscle perfusion: its measurement and role in metabolic regulation. *Diabetes.* (2012) 61:2661–8. doi: 10.2337/db12-0271
2. Saltin B. Exercise hyperaemia: magnitude and aspects on regulation in humans. *J Physiol.* (2007) 583:819–23. doi: 10.1113/jphysiol.2007.136309
3. Delp MDL, Laughlin MH. Regulation of skeletal muscle perfusion during exercise. *Acta Physiol Scand.* (1998) 162:411–9. doi: 10.1046/j.1365-201X.1998.0324e.x
4. Raynaud JS, Duteil S, Vaughan JT, Hennel F, Wary C, Leroy-Willig A, et al. Determination of skeletal muscle perfusion using arterial spin labeling NMRI: validation by comparison with venous occlusion plethysmography. *Magn Reson Med.* (2001) 46:305–11. doi: 10.1002/mrm.1192
5. Englund EK, Rodgers ZB, Langham MC, Mohler ER, 3rd, Floyd TF, Wehrli FW. Simultaneous measurement of macro- and microvascular blood flow and oxygen saturation for quantification of muscle oxygen consumption. *Magn Reson Med.* (2018) 79:846–55. doi: 10.1002/mrm.26744
6. Joyner MJ, Casey DP. Regulation of increased blood flow (hyperemia) to muscles during exercise: a hierarchy of competing physiological needs. *Physiol Rev.* (2015) 95:549–601. doi: 10.1152/physrev.00035.2013
7. Korthuis RJ. *Chapter 4, Exercise Hyperemia and Regulation of Tissue Oxygenation During Muscular Activity*. San Rafael, CA: Morgan & Claypool Life Sciences (2011).
8. Le Bihan D, Breton E, Lallemand D, Aubin ML, Vignaud J, Laval-Jeantet M. Separation of diffusion and perfusion in intravoxel incoherent motion MR imaging. *Radiology.* (1988) 168:497–505. doi: 10.1148/radiology.168.2.3393671
9. Englund EK, Reiter DA, Shahidi B, Sigmund EE. Intravoxel incoherent motion magnetic resonance imaging in skeletal muscle: review and future directions. *J Magn Reson Imag.* (2022) 55:988–1012. doi: 10.1002/jmri.27875
10. Le Bihan D. What can we see with IVIM MRI? *Neuroimage.* (2019) 187:56–67. doi: 10.1016/j.neuroimage.2017.12.062
11. Shahidi B, Hubbard JC, Gibbons MC, Ruoss S, Zlomislic V, Allen RT, et al. Lumbar multifidus muscle degenerates in individuals with chronic degenerative lumbar spine pathology. *J Orthop Res.* (2017) 35:2700–6. doi: 10.1002/jor.23597

12. Shahidi B, Parra CL, Berry DB, Hubbard JC, Gombatto S, Zlomislic V, et al. Contribution of lumbar spine pathology and age to paraspinal muscle size and fatty infiltration. *Spine*. (2016) 42:616–23. doi: 10.1097/BRS.0000000000001848
13. Teichtahl AJ, Urquhart DM, Wang Y, Wluka AE, Wijethilake P, O'Sullivan R, et al. Fat infiltration of paraspinal muscles is associated with low back pain, disability and structural abnormalities in community-based adults. *Spine J*. (2015) 15:1593–601. doi: 10.1016/j.spinee.2015.03.039
14. Kim CY, Choi JD, Kim SY, Oh DW, Kim JK, Park JW. Comparison between muscle activation measured by electromyography and muscle thickness measured using ultrasonography for effective muscle assessment. *J Electromyogr Kinesiol*. (2014) 24:614–20. doi: 10.1016/j.jelekin.2014.07.002
15. Donisch EW, Basmajian JV. Electromyography of deep back muscles in man. *Am J Anat*. (1972) 133:25–36. doi: 10.1002/aja.1001330103
16. Sommerich CM, Joines SM, Hermans V, Moon SD. Use of surface electromyography to estimate neck muscle activity. *J Electromyogr Kinesiol*. (2000) 10:377–98. doi: 10.1016/S1050-6411(00)00033-X
17. Shahidi B, Behun JJ, Berry DB, Raiszadeh K, Englund EK. Intravoxel incoherent motion imaging predicts exercise-based rehabilitation response in individuals with low back pain. *NMR Biomed*. (2021) 34:e4595. doi: 10.1002/nbm.4595
18. Nguyen A, Ledoux JB, Omoumi P, Becce F, Forget J, Federau C. Application of intravoxel incoherent motion perfusion imaging to shoulder muscles after a lift-off test of varying duration. *NMR Biomed*. (2016) 29:66–73. doi: 10.1002/nbm.3449
19. Nguyen A, Ledoux JB, Omoumi P, Becce F, Forget J, Federau C. Selective microvascular muscle perfusion imaging in the shoulder with intravoxel incoherent motion (IVIM). *Magn Reson Imag*. (2017) 35:91–7. doi: 10.1016/j.mri.2016.08.005
20. Morvan D. In vivo measurement of diffusion and pseudo-diffusion in skeletal muscle at rest and after exercise. *Magn Reson Imag*. (1995) 13:193–9. doi: 10.1016/0730-725X(94)00096-L
21. Filli L, Boss A, Wurnig MC, Kenkel D, Andreisek G, Guggenberger R. Dynamic intravoxel incoherent motion imaging of skeletal muscle at rest and after exercise. *NMR Biomed*. (2015) 28:240–6. doi: 10.1002/nbm.3245
22. Adelnia F, Shardell M, Bergeron CM, Fishbein KW, Spencer RG, Ferrucci L, et al. Diffusion-weighted MRI with intravoxel incoherent motion modeling for assessment of muscle perfusion in the thigh during post-exercise hyperemia in younger and older adults. *NMR Biomed*. (2019) 32:e4072. doi: 10.1002/nbm.4072
23. Mastropietro A, Porcelli S, Cadioli M, Rasica L, Scalco E, Gerevini S, et al. Triggered intravoxel incoherent motion MRI for the assessment of calf muscle perfusion during isometric intermittent exercise. *NMR Biomed*. (2018) 31:e3922. doi: 10.1002/nbm.3922
24. Jungmann PM, Pfirrmann C, Federau C. Characterization of lower limb muscle activation patterns during walking and running with intravoxel incoherent motion (IVIM) MR perfusion imaging. *Magn Reson Imag*. (2019) 63:12–20. doi: 10.1016/j.mri.2019.07.016
25. Riexinger A, Laun FB, Hoger SA, Wiesmueller M, Uder M, Hensel B, et al. Effect of compression garments on muscle perfusion in delayed-onset muscle soreness: a quantitative analysis using intravoxel incoherent motion MR perfusion imaging. *NMR Biomed*. (2021) 34:e4487. doi: 10.1002/nbm.4487
26. Federau C, Kroismayr D, Dyer L, Farshad M, Pfirrmann C. Demonstration of asymmetric muscle perfusion of the back after exercise in patients with adolescent idiopathic scoliosis using intravoxel incoherent motion (IVIM) MRI. *NMR Biomed*. (2020) 33:e4194. doi: 10.1002/nbm.4194
27. Hiepe P, Gussew A, Rzanny R, Anders C, Walther M, Scholle HC, et al. Interrelations of muscle functional MRI, diffusion-weighted MRI and (31) P-MRS in exercised lower back muscles. *NMR Biomed*. (2014) 27:958–70. doi: 10.1002/nbm.3141
28. Andersson JLR, Skare S, Ashburner J. How to correct susceptibility distortions in spin-echo echo-planar images: application to diffusion tensor imaging. *NeuroImage*. (2003) 20:870–88. doi: 10.1016/S1053-8119(03)00336-7
29. Smith SM, Jenkinson M, Woolrich MW, Beckmann CF, Behrens TE, Johansen-Berg H, et al. Advances in functional and structural MR image analysis and implementation as FSL. *Neuroimage*. (2004) 23(Suppl. 1):S208–19. doi: 10.1016/j.neuroimage.2004.07.051
30. Manjon JV, Coupe P, Concha L, Buades A, Collins DL, Robles M. Diffusion weighted image denoising using overcomplete local PCA. *PLoS ONE*. (2013) 8:e73021. doi: 10.1371/journal.pone.0073021
31. Filli L, Wurnig MC, Luechinger R, Eberhardt C, Guggenberger R, Boss A. Whole-body intravoxel incoherent motion imaging. *Eur Radiol*. (2015) 25:2049–58. doi: 10.1007/s00330-014-3577-z
32. Le Bihan D, Turner R. The capillary network: a link between IVIM and classical perfusion. *Magn Reson Med*. (1992) 27:171–8. doi: 10.1002/mrm.1910270116
33. Berry DB, Padwal J, Johnson S, Parra CL, Ward SR, Shahidi B. Methodological considerations in region of interest definitions for paraspinal muscles in axial MRIs of the lumbar spine. *BMC Musculoskelet Disord*. (2018) 19:135. doi: 10.1186/s12891-018-2059-x
34. Lyu X, Gao Y, Liu Q, Zhao H, Zhou H, Pan S. Exercise-induced muscle damage: multi-parametric MRI quantitative assessment. *BMC Musculoskelet Disord*. (2021) 22:239. doi: 10.1186/s12891-021-04085-z
35. Fisher MJ, Meyer RA, Adams GR, Foley JM, Potchen EJ. Direct relationship between proton T2 and exercise intensity in skeletal muscle MR images. *Invest Radiol*. (1990) 25:480–5. doi: 10.1097/00004424-199005000-00003
36. Haddock B, Holm S, Poulsen JM, Enevoldsen LH, Larsson HB, Kjaer A, et al. Assessment of muscle function using hybrid PET/MRI: comparison of (18)F-FDG PET and T2-weighted MRI for quantifying muscle activation in human subjects. *Eur J Nucl Med Mol Imag*. (2017) 44:704–11. doi: 10.1007/s00259-016-3507-1
37. Haddock B, Hansen SK, Lindberg U, Nielsen JL, Frandsen U, Aagaard P, et al. Physiological responses of human skeletal muscle to acute blood flow restricted exercise assessed by multimodal MRI. *J Appl Physiol 1985*. (2020) 129:748–59. doi: 10.1152/japplphysiol.00171.2020
38. Rockel C, Akbari A, Kumbhare DA, Noseworthy MD. Dynamic DTI (dDTI) shows differing temporal activation patterns in post-exercise skeletal muscles. *MAGMA*. (2017) 30:127–38. doi: 10.1007/s10334-016-0587-7
39. Froeling M, Oudeman J, Strijkers GJ, Maas M, Drost MR, Nicolay K. Muscle changes detected with diffusion-tensor imaging after long-distance running. *Radiology*. (2015) 274:548–62. doi: 10.1148/radiol.14140702
40. Damon BM, Wadington MC, Hornberger JL, Lansdown DA. Absolute and relative contributions of BOLD effects to the muscle functional MRI signal intensity time course: effect of exercise intensity. *Magn Reson Med*. (2007) 58:335–45. doi: 10.1002/mrm.21319
41. Muller MD, Li Z, Sica CT, Luck JC, Gao Z, Blaha CA, et al. Muscle oxygenation during dynamic plantar flexion exercise: combining BOLD MRI with traditional physiological measurements. *Physiol Rep*. (2016) 4:e13004. doi: 10.14814/phy2.13004
42. Bourne MN, Williams MD, Opar DA, Al Najjar A, Kerr GK, Shield AJ. Impact of exercise selection on hamstring muscle activation. *Br J Sports Med*. (2017) 51:1021–8. doi: 10.1136/bjsports-2015-095739

Conflict of Interest: The authors declare that the research was conducted in the absence of any commercial or financial relationships that could be construed as a potential conflict of interest.